Effect of Melt Annealing on the Phase Structure and Rheological Behavior of Propylene–Ethylene Copolymers

Vanesa De La Torre, Jorge A. Rodríguez Fris, Marcelo D. Failla, Lidia M. Quinzani
Planta Piloto de Ingeniería Química, UNS/CONICET, C.C. 717, (8000) Bahía Blanca, Argentina

The morphological and rheological properties of a commercial propylene-ethylene copolymer (PEC) and a series of blends with different concentrations of poly (ethylene-*co*-propylene) are investigated. The blends are prepared mixing PEC with fractions obtained from it by solvent extraction. The phase structure of samples exposed to different thermal and mechanical histories was analyzed using scanning electron microscopy. The linear viscoelastic properties of the molten polymers were measured using different test sequences that include dynamic frequency and time sweeps. The phase structure of most blends changes dramatically with time when the polymers are kept in the molten state due to the coalescence of the domains. For example, the initial morphology of PEC which presents domains of ~1 μm diameter changes to regions of more than 10 μm of average diameter after 90 min at 178°C at rest. Coincidentally, the dynamic moduli of the blends change during annealing reaching values that depend on the mechanical history. For example, the elastic modulus of PEC increases ~32% during a dynamic time sweep of 45 min using a frequency of 0.1 s^{-1}, while it decreases ~18% when a frequency of 1 s^{-1} is applied. Moreover, the modulus measured at 0.1 s^{-1} of samples annealed at rest during 45 min is ~58% larger than that of the fresh material. POLYM. ENG. SCI., 47:912–921, 2007. © 2007 Society of Plastics Engineers

INTRODUCTION

Since the production of polypropylene (PP) began in 1957, great research effort has been directed towards the improving of the low temperature impact behavior of this material. The most successful procedures found so far are the mechanical blending of PP with polyethylene (PE) or elastomers such as ethylene–propylene copolymer (EPR), and the copolymerization of PP with ethylene or dienes [1, 2]. An effective, commercially used copolymerization process consists of the homopolymerization of propylene in a first stage followed by the copolymerization of ethylene and propylene in a second stage. The propylene–ethylene copolymers obtained in this way consist basically of PP and a large variety of poly(ethylene-*co*-propylene) molecules with different monomer ratios. These materials present a complex morphology both in the solid and the molten state because of the limited miscibility of the components. Basically, the alloys present poly(ethylene-*co*-propylene) domains embedded in a matrix composed mainly by PP. The domains present a crystallizable fraction consisting of polyethylene and ethylene-rich molecules and an amorphous fraction composed of random copolymer molecules [3–7]. The properties of these materials are strongly affected by both the matrix and dispersed phase composition and by the morphology, which is mainly determined by the interaction between components and the processing conditions [6–9]. Moreover, the flow may affect the morphology changing the degree and type of dispersion on a local level, and the morphology generated by a given flow condition may not be stable when the molten blend is brought to a motionless or a low-stress state. Variations of the phase organization of the blend with time may then be observed [9]. The comprehension of the time dependence of the morphology of multiphase materials while at rest and during processing is very important for the understanding of the performance of the final products and the applications of the materials.

The change in size and composition of the phases of immiscible polymeric systems with time may be caused by the migration of one or more of the components, and by the coalescence and breakup of the domains. A considerable amount of work has been done to analyze the effects of flow on the morphology and stability of polymer blends [9]. However, only a few studies may be found in the literature that analyze the effect of melt annealing and postprocessing conditions on the morphology and properties of blends [10–18]. Cheng et al. [10] analyzed the effect of quiescent annealing at 270°C on blends of polycarbonate with various brittle polymers and impact modifiers simulating certain conditions that can occur during molding or extrusion. These authors found that a significant change in blend morphology occurs in the first 2 min of melt annealing and that the dispersed

phase shows significant size growth with time. In some cases of ternary blends, they observed that the cocontinuity generated during flow is lost during the melt annealing. Chen et al. [11] observed similar behavior using blends of nylon with polyethylenes and polystyrenes. Xie et al. [12] detected the development of gradient-phase morphology in a molten blend of PP and ethylene-vinyl acetate copolymer with an initial uniform distribution of dispersed phase. The size of the particles was observed to increase gradually towards the sample surface with increasing annealing time and temperature. Fortelný and Zivný [13] derived a theory for the coalescence of droplets dispersed in molten quiescent polymer blends (with more than 0.1% of dispersed phase) considering Van der Waals type of driving forces for coalescence. They conclude that different combinations of interface mobility and driving forces for coalescence can lead to the same shape of the time dependence of droplet radius. The theory predicts higher rates of coalescence than the ones determined experimentally for a model system of low-density polyethylene dispersed in polystyrene [14]. The radius of the dispersed domains grows with time as $t^{1/3}$. The theory fails when the driving forces for coalescence are weak. Li et al. [15] analyzed the evolution of the morphology of PP/PE/EPR blends during quiescent annealing at 175°C using different EPR concentrations. According to these authors, the dispersed domains grew in size during the annealing and the presence of EPR in the blends retarded that growth. Feng and Hay [16] studied phase separation in a commercial propylene–ethylene copolymer with 8 mol% of global ethylene content and found that the size of the discrete domains increases with annealing time in the melt. According to these authors, the observed reduction in the number of dispersed domains and the consequent increase in domain sizes, is mainly due to Ostwald ripening (minimization of total energy by reduction of interfacial area) and follows the theoretical prediction with time of $d \sim t^{1/3}$ and $N \sim t^{-1}$. Here d is the average drop diameter and N is the number of particles.

The relationship between morphology and flow behavior of blends is reciprocal in the sense that flow affects the phase structure and alterations in the structure also produce changes in the rheological response of polymer blends. A large amount of information can be found in the literature about morphological and rheological properties of immiscible polymer blends [9]. The relationship between these properties is very complex and it cannot be generalized. The main factors that affect the phase structure of polymer blends are: the concentration of dispersed domains, the rheological properties of the components and the interactions between them, the magnitude and rate of the applied deformation, the presence of external forces like gravity, and the processing conditions. Polymer blends usually exhibit very slow relaxation processes that are affected by the interfacial tension and the concentration, size and shape of the dispersed domains [9, 19–26]. The energy associated with these relaxation processes affects the dynamic response of the blends and is normally perceived as an increase in the elastic modulus at low frequencies.

Given the lack of information on the phase structure and rheological behavior of heterophasic propylene–ethylene copolymers, we carried out the present work to analyze the time dependence of the morphology and the rheological properties of molten copolymers with different poly(ethylene-*co*-propylene) content. The materials were generated by blending a commercial copolymer with different amounts of fractions separated from it by toluene extraction. The effect of the annealing process on molten materials kept at rest and on samples simultaneously subjected to different deformation histories is analyzed.

EXPERIMENTAL

Materials

The propylene–ethylene copolymer was supplied by Petroquímica Cuyo S.A.I.C. (Mendoza, Argentina). It was produced via sequential polymerization process. This polymer, which is identified in the paper as PEC, has a global ethylene content of 16.4 mol%. This value was estimated from the method proposed by Paroli using area ratios of infrared peaks [27]. The weight- and number-average molecular weights of PEC are 298,000 and 69,000 g/mol respectively. They were estimated using gel permeation chromatography following the standard procedure using Mark-Howink coefficients for polypropylene. The runs were performed at 140°C in a Waters 150-C ALP/GPC system equipped with a set of 10 μm PLGel columns (Polymer Labs) having nominal pore size of 10^6, 10^4, and 500 Å, using 1,2,4-trichlorobenzene as solvent.

Two fractions were obtained from PEC by selective extraction with toluene at 90°C. This procedure separates a toluene soluble fraction (S) from the rest of the polymer, which is left as a residue (R). The soluble part, which is about 12 wt% of the total mass, contains most of the amorphous poly(ethylene-*co*-propylene) originally in PEC and a small fraction of atactic PP from the matrix [4]. Both fractions were characterized using differential scanning calorimetry employing a Perkin Elmer system Pyris 1. A heating rate of 10°C/min was used in the range of 30–180°C on samples previously subjected to a cycle of melting and crystallization to erase the thermal history. No melting endotherm was observed in the thermogram of S indicating that this fraction contains essentially amorphous material. In the case of R, melting peaks were observed at 120 and 165°C, indicating that this material is mainly formed by polypropylene and ethylene-rich molecules. Infrared spectroscopic results reveal that S contains ~50 mol% of ethylene. This result means that ~8 wt% of R is made of polyethylene and ethylene-rich molecules. The composition of the copolymer is similar to that of the

materials characterized by Zacur et al. using temperature-rising elution fractionation (TREF) [4].

A set of materials were prepared by blending the original PEC with different amounts of either S or R. The mixing was done in a Brabender mixer (Plastograph) equipped with a 55 cm³ bowl and roller blades. The mixing conditions used in all the cases were 200°C, 30 rpm of blade speed, and 10 min of mixing time. Nitrogen atmosphere was used to avoid oxidation of the polymer. The heterophasic polymers PEC and R were also processed using the conditions that were mentioned above to ensure that all the materials used in the rheological study had the same initial thermal and deformation histories. The molten polymers were removed from the mixer bowl and rapidly compress-molded to obtain plates of about 1.5 mm thick. Discs of 25 mm diameter were cut from these plates to be used in the rheological study. S was not processed in the mixer before the rheological characterization. Table 1 displays the proportion of PEC, S, and R used to prepare each blend, as well as the nomenclature that identifies the generated alloys. The final ethylene content of the blends is between 13 and 19 mol% while the amount of amorphous poly(ethylene-*co*-propylene) goes from 4 wt% in PEC/R7 up to 20 wt% in PEC/S1.

Morphological Characterization

The phase structure of the copolymers was studied analyzing fracture surfaces by scanning electron microscopy (SEM) in a Jeol JSM-35CF system with 6 kV acceleration voltage. The analyzed specimens were ~1.5 mm thick samples that were fractured at liquid nitrogen temperature. Phase contrast was achieved by sinking the specimens in toluene for ~1 h to extract the soluble material S in the surface. The resulting surfaces were finally coated with a thin layer of gold for SEM examination.

Rheological Characterization

The rheological characterization was carried out under nitrogen atmosphere using a rotational rheometer from Rheometrics (model RDA-II). The elastic modulus, $G'(\omega)$, and the viscous modulus, $G''(\omega)$, were measured at 178°C in small-amplitude oscillatory shear flow experiments. This type of flow is normally used to study the rheological behavior of blends due to the relatively small effects that it has on the morphology [9]. Measurements were performed using 25 mm parallel plate fixtures and samples of ~1.5 mm thick. All the runs were repeated using at least two different samples of each material with similar thermal history. Excellent agreement between the results was found in all the cases. Along the paper, we use the elastic modulus, $G'(\omega)$, and the dynamic viscosity, $\eta'(\omega) = G''(\omega)/\omega$, to represent the results.

Three types of tests were performed: dynamic strain sweep (DSS), dynamic frequency sweep (DFS), and dynamic-time sweep (DTS). The DSS were used to deter-

TABLE 1. Composition and estimated final concentration of soluble material of the blends expressed as weight percentages.

	PEC (wt%)	S (wt%)	R (wt%)	Global content of S (wt%)
PEC/S1	91	9	—	20
PEC/S0	95	5	—	16
PEC	100	—	—	12
PEC/R1	91	—	9	11
PEC/R2	77	—	23	9
PEC/R5	67	—	33	8
PEC/R7	30	—	70	4

mine the extent of the linear viscoelastic region of each polymer. A constant rate of 10 s^{-1} was used in all the DSS runs. The DFS were applied in the range from 0.04 to 400 s^{-1} using a strain previously selected in the linear viscoelastic regime. This test lasts ~20 min. The DTSs were applied at 178°C during a period of 45 min using a constant frequency of 0.1 or 1 s^{-1}. The tests will be further described in the following sections.

RESULTS AND DISCUSSION

Phase Structure of PEC

Figure 1 displays four micrographs of samples of PEC that have been subjected to different thermo-mechanical histories. These pictures have been selected from among many micrographs as representative of the observed coalescence phenomenon. In all of them, the dispersed cavities were produced by the poly(ethylene-*co*-propylene) extracted by the toluene while the quasispherical particles that lie on the surface or inside the cavities are formed by the ethylene-rich molecules. Some of the particles originally in the fracture surface may have been swept away by the solvent during the extraction process.

The micrographs in Fig. 1 clearly show the progressive change of the phase structure of PEC with time when the material is subjected to annealing at 178°C. The initial polymer (Fig. 1a) presents spherical domains of about 1 μm of diameter homogeneously dispersed in the matrix. These domains grow in size when the sample is kept at rest in the molten state. For example, after 8 min of annealing (see Fig. 1b), the domains reached a diameter of about 4 μm. A closer examination of the structure shows evidence of domain coalescence through the bundle of holes and of particles that can be seen in some zones of the surface. The coalescence and growth of the dispersed phase continue when the material is kept longer periods of time in the melt. Figures 1c and d, which correspond to samples that have been at 178°C for 90 and 180 min (respectively), show domains and holes larger than 10 μm. Furthermore, the dramatic increase in size of the ethylene-rich areas is so large that, after 3 h of annealing, the appearance of the phase structure even suggests cocontinuity. The evolution of the microstructure is
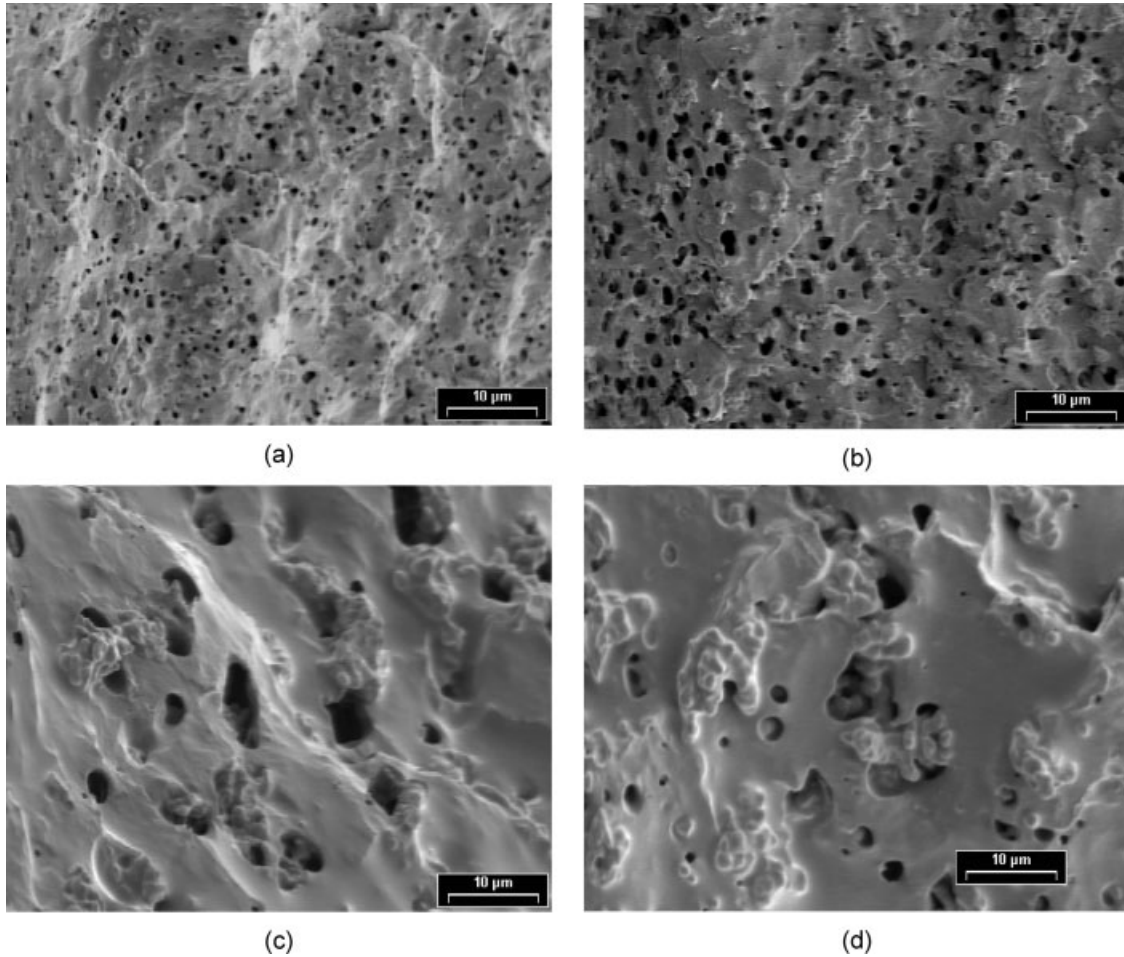
FIG. 1. SEM micrographs of rapidly cooled samples of PEC after mixing in the blender (a) and after being at rest at 178°C for 8 min (b), 90 min (c), and 180 min (d). Size of the observed zones: 47×60 μm.

a consequence of the tendency of immiscible systems to reduce the surface energy associated with interfacial area. This process is realized by a coalescence mechanism where the coarsening might occur by small domains that impinge on each other by translational diffusion [13].

Initial Dynamic Behavior

Figure 2 shows the dynamic viscosity $\eta'(\omega)$ and the elastic modulus $G'(\omega)$ of PEC and the fractions S and R. Fresh samples were used in all the experiments. The dynamic moduli of PEC may correspond to a material with morphology similar to the one shown in Fig. 1b since ~10 min has elapsed by the time the first data point of a DFS is obtained (at 0.04 s^{-1}). The large values of the dynamic moduli of S indicate that this is a material of relatively large molecular weight. Similar behavior has been found in the literature for equivalent materials [7, 8]. The data of PEC agree with the typical rheological behavior of a polymeric blend. At large frequencies, both η' and G' are close to the corresponding parameters of R, which constitutes 88 wt% of PEC. Meanwhile, at small frequencies, the dynamic moduli of PEC are larger than

the ones of both S and R. This is a behavior frequently found in immiscible blends [9, 19–26] where the slow relaxation processes of the interfaces add to the molecular
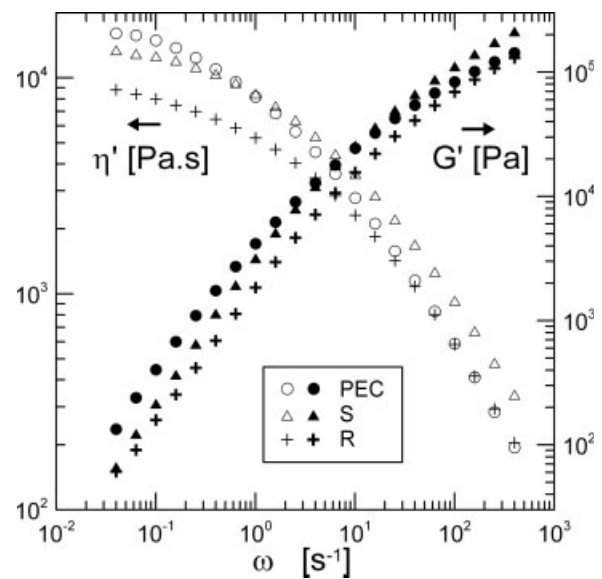

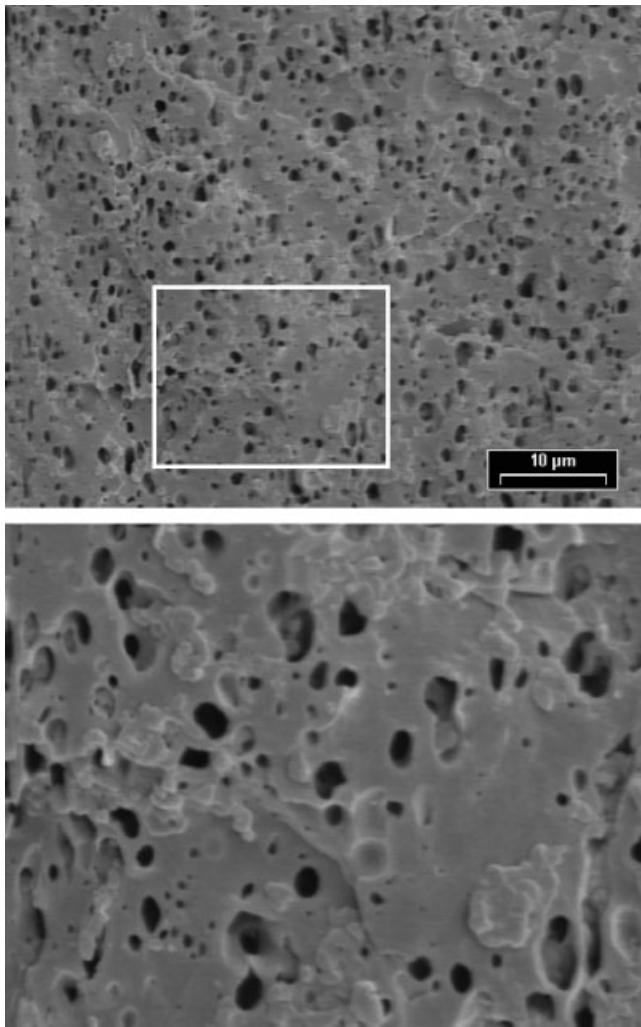FIG. 2. Dynamic viscosity and elastic modulus of PEC, S and R at 178°C.

FIG. 3. SEM micrographs of a fresh sample of PEC/S1. Size of the displayed zones: 47 × 60 μm (top) and 16.5 × 21 μm (bottom).

relaxation of the polymer. These relaxation processes should affect more the elastic than the viscous properties of a polymeric blend. In the present case, the increase in the viscous modulus is larger than the one that is usually observed in two-component blends. Evidence of the existence of a blend can also be found in the rheological behavior of the residual material. The evolution of the elastic modulus of R, which is form by the PP and the ethylene-rich molecules, shows the typical increase at low frequencies due to the effect of the presence of an interface. The attempt of using the emulsion model of Palierne [28] to predict the rheological behavior of PEC as a blend of S and R gave unsatisfactory results. This is a predictable conclusion since R is not a homogeneous polymer and PEC is not a binary mixture with dispersed domains. Brahimi et al. [29], who have studied blends of PE, polystyrene, and hydrogenated styrene-butadiene copolymer, made an equivalent attempt. They also found that the predictions of the emulsion model of Palierne did not agree with the rheological behavior of the complex blends.

The phase morphology and the rheological response of fresh samples of the blends were also studied and compared. The analyzed materials differ basically in the concentration of poly(ethylene-*co*-propylene), the rubbery material. When the amount of S in the blends is small, this polymer locates in the interphase between the PP and ethylene-rich material, compatibilizing these two phases [3–7]. As the concentration of S increases, part of this polymer may exist as a separated phase in the PP matrix. Li et al. [15], using confocal fluorescence microscopy, observed the presence of EPR domains in a 85/15 ratio PP/PE matrix for EPR concentrations larger than 10 wt%. For smaller concentrations of rubbery material (2–5 wt%), this polymer is localized in the interphase between the PE droplets and the PP matrix. As an example of the initial phase structure of our blends, Figs. 3 and 4 display the morphology of PEC/S1 and PEC/R7 respectively, which are the materials with the largest (∼20 wt%) and the smallest (∼4 wt%) concentration of S respectively. Each figure displays the morphology captured with two magni-
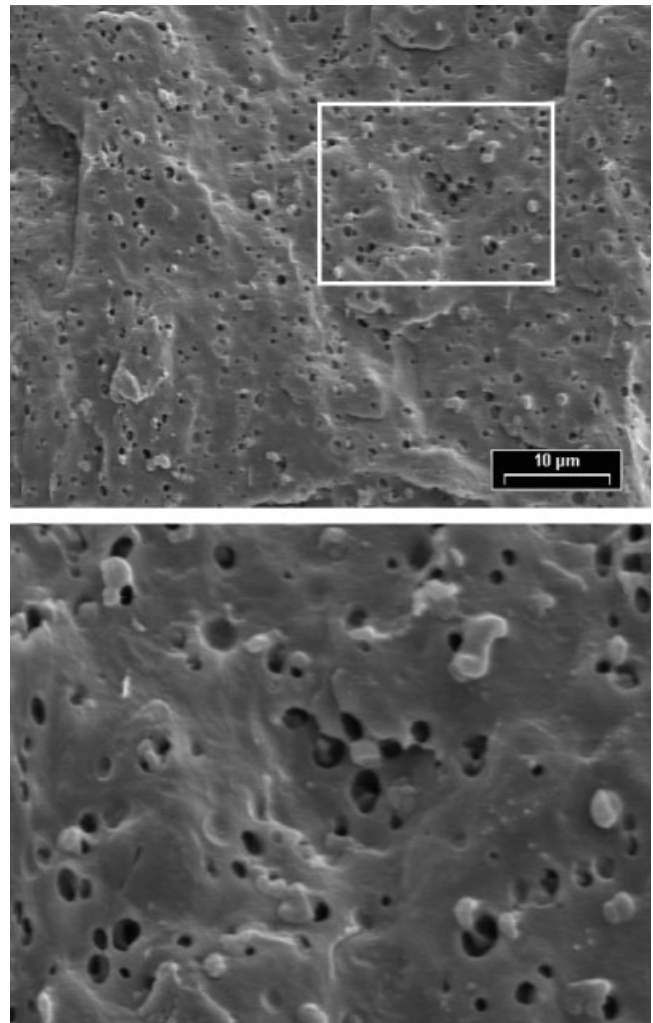

FIG. 4. SEM micrographs a of fresh sample of PEC/R7. Size of the displayed zones: 47 × 60 μm (top) and 16.5 × 21 μm (bottom).
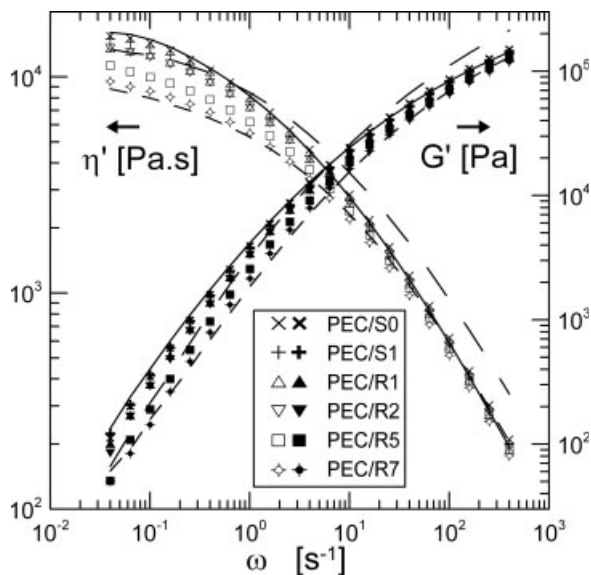
FIG. 5. Dynamic viscosity and elastic modulus of fresh samples of all the blends at 178°C. Solid lines: PEC; long dashed lines: S; short dashed lines: R.

fications (2000× and 6000×). These photographs can also be compared with the micrograph of the initial phase structure of PEC presented in Fig. 1a. The surface of PEC/R7 exhibits disperse quasi-spherical holes and particles of ethylene-rich polymer, while that of PEC/S1 contains bundles of particles and larger holes left by the dissolved rubbery material. Some of the particles originally in the analyzed fracture-surface may have been swept away by the solvent during the extraction process used to obtain phase contrast. This effect should be more noticeable as the concentration of S increases.

Figure 5 displays the initial dynamic parameters of the blends. The dynamic behavior of PEC, S and R are also included in this Figure to facilitate the comparison. At high frequency, all the materials present elastic and viscous moduli very similar to that of R (the residual material that constitutes 80 wt% or more of the copolymers). At low frequency, were the morphology of the blends has a larger impact, different values of the moduli can be observed. The PEC/Ri blends that were obtained adding the residual material to PEC present dynamic moduli that gradually decrease as the concentration of R increases. The relatively low value of the viscous and elastic moduli of R produces the gradual decrease of the moduli of the blends with respect to those of PEC. However, the addition of amorphous poly(ethylene-co-propylene) material (S) to PEC does not follow that trend and it does not produce a further increase of the dynamic moduli. Actually, the original copolymer, PEC, presents the largest moduli at low frequency while the blends that were obtained adding 5 and 9 wt% of S to PEC display parameters slightly smaller. The rheological response of the analyzed materials agree with the fact that they are blends of PEC and either S or R that do not necessarily have the phase mor-

phology of commercial copolymers of equivalent composition.

Transient Rheological Behavior

The transient rheological behavior of the blends is analyzed at 178°C using different sequences of rheological tests. All the sequences begin with a DFS that lasts ~20 min and proceed with either a DTS or an equivalent period of no deformation. Another DFS is applied at the end of the test sequences. The DTS consists of 45 min of oscillatory shear flow at constant frequency. The data obtained in the initial DFS are the ones already shown in Fig. 5.

Behavior of PEC. Figure 6 shows the parameters $\eta'(\omega)$ and $G'(\omega)$ of PEC after different mechanical histories. The full lines correspond to the dynamic moduli obtained in the initial DFS (already shown in Fig. 2). Each sequence of "initial DFS—period of annealing with or without oscillatory flow–final DFS" was performed on a fresh sample of PEC. As it may be observed in the Figure, the final rheological parameters depend on the thermo-mechanical history applied to the sample. The largest values are obtained when the material has been kept in the molten state with no deformation. Furthermore, the largest increase in the value of the dynamic data is obtained when the elapsed time is the longest (compare curves obtained after 45 and 90 min of no deformation). When the material is subjected to 45 min of continuous oscillatory shear flow with a small frequency (0.1 s^{-1}), the parameters measured in the final DFS are also larger than the original ones although not as large as
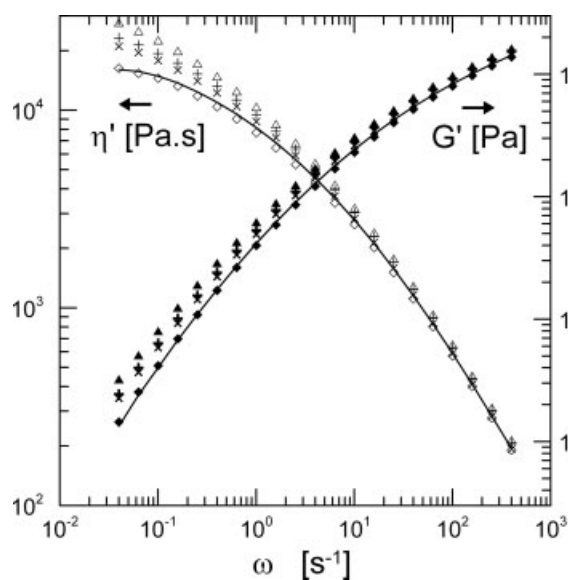

FIG. 6. Dynamic viscosity and elastic modulus of samples of PEC subjected to an initial DFS followed by different mechanical histories at 178°C. (△): 90 min at rest; (+): 45 min at rest; (×): 45 min at 0.1 s^{-1}; (◆): 45 min. at 1 s^{-1}.

those of the samples kept at rest. However, if the material is constantly deformed at a frequency of $1 \ s^{-1}$, the dynamic moduli of the annealed polymer are smaller than the parameters of the fresh sample. In all the cases, the difference between the final values of G' and η' and the original ones increases as the frequency decreases. This phenomenon agrees with the fact that the phase structure of a blend affects mainly the slow relaxation processes.

The elastic modulus of PEC and the fractions R and S measured during the DTS are presented in Fig. 7. These data were obtained from samples that have been subjected to an initial DFS. The curves of $G''(t)$ of the three polymers are similar to those of G' and display the same trends. As it may be observed, the parameters of the soluble material, S, remain constant during the tests while the moduli of the heterogeneous R display a slight dependency with time, at least at $\omega = 1 \ s^{-1}$. Meanwhile, the dynamic parameters of PEC increase when a frequency of $0.1 \ s^{-1}$ is used and they decrease at $1 \ s^{-1}$. In this case, the decrease is larger than the one observed in Fig. 6. The reason for this discrepancy is that the data of the final DFS actually correspond to a material that has been further annealed after the DTS, in a practically quiescent state, because of the time it takes to measure the moduli at low frequencies. This further annealing produces an increase back of the parameters. Although more noticeable in the data measured using a frequency of $1 \ s^{-1}$, this is an effect that is present in all the results of Fig. 6. The rheological behavior of R and S shown in Fig. 7 indicates that polymer degradation during the transient tests is negligible. The frequency of $1 \ s^{-1}$ is the largest one used in the DTS because evidence of viscous heating was found when a frequency of $10 \ s^{-1}$ was used. The change in the rheological parameters of PEC may be caused by the combined effects of a gradual modification of the phase structure of the polymer during the annealing and the gradual change of the composition of molecular chains at the interface. This last effect in turn changes the strength of the interface which in turn changes the rheological behavior. Furthermore, according to the results, these modifications are affected by the applied mechanical history.

The rheological study was complemented with the examination of the phase structure of the polymers using SEM. The morphological study was carried out on samples used in the rheological study and that were carefully cooled to room temperature after the DTS or the annealing at rest. No final DFS is applied to these samples. The cooling was done as fast as possible (in ~1 min) keeping the material under no tension to avoid deformation. The polymeric disks were later broken in two halves following the procedure commented in the Experimental section. All the annealed materials display dispersed domains larger than those seen in the fresh samples of PEC coming from the mixer (Fig. 1a). With one exception, the images of the phase structure of the annealed materials turn out to be practically indistinguishable, regardless of
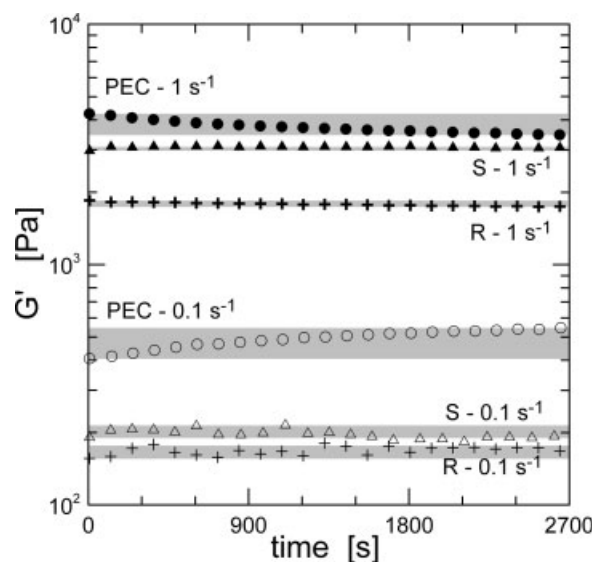

FIG. 7.   Elastic modulus of PEC, R, and S measured in dynamic time sweeps at 178°C. The gray zones are the regions determined by the minimum and maximum values of G' measured in each case.

the applied deformation history and of the location in the fracture-surfaces. In all the cases, the phase structure looked like the image shown in Fig. 8a and c, which corresponds to the material used in the DTS with $\omega = 1 \ s^{-1}$ and near the center of the disk. The photographs that suggest a difference in structure are the ones that correspond to the material kept 45 min under oscillatory flow at $1 \ s^{-1}$ and were taken near the edge of the disc, at $r \cong R$ (see Fig. 8b and d). The domains that appear in this area of the copolymer seem to be a little smaller and more homogeneously dispersed.

Clearly, the rheological characterization has a sensibility to details of the phase and interphase structures of the copolymer that the microscopic method used in the study does not posses. The fact that the structures observed by SEM might not represent exactly the phase organization during flow due to the cooling and extraction processes applied to the samples, it must also be taken into account.

Behavior of the Blends.   The effect of the thermo-rheological history on the dynamic properties of the blends is qualitatively similar to that observed in PEC in all the cases except PEC/R7; that is, the dynamic moduli change during the annealing and the largest values are observed in samples annealed at rest during 90 min. Figure 9 shows the elastic modulus $G'(\omega)$ of all the materials measured during the dynamic time weeps with $\omega = 0.1$ and $1 \ s^{-1}$. These tests were performed after an initial DFS. The data corresponding to PEC are also included in the Figure. Although not shown here, the curves of $G''(\omega)$ display the same qualitative behavior than those of the elastic modulus. For a frequency of $0.1 \ s^{-1}$, the rheological properties of the copolymers increase with time, except in the case of PEC/R7 that has properties that remain constant in
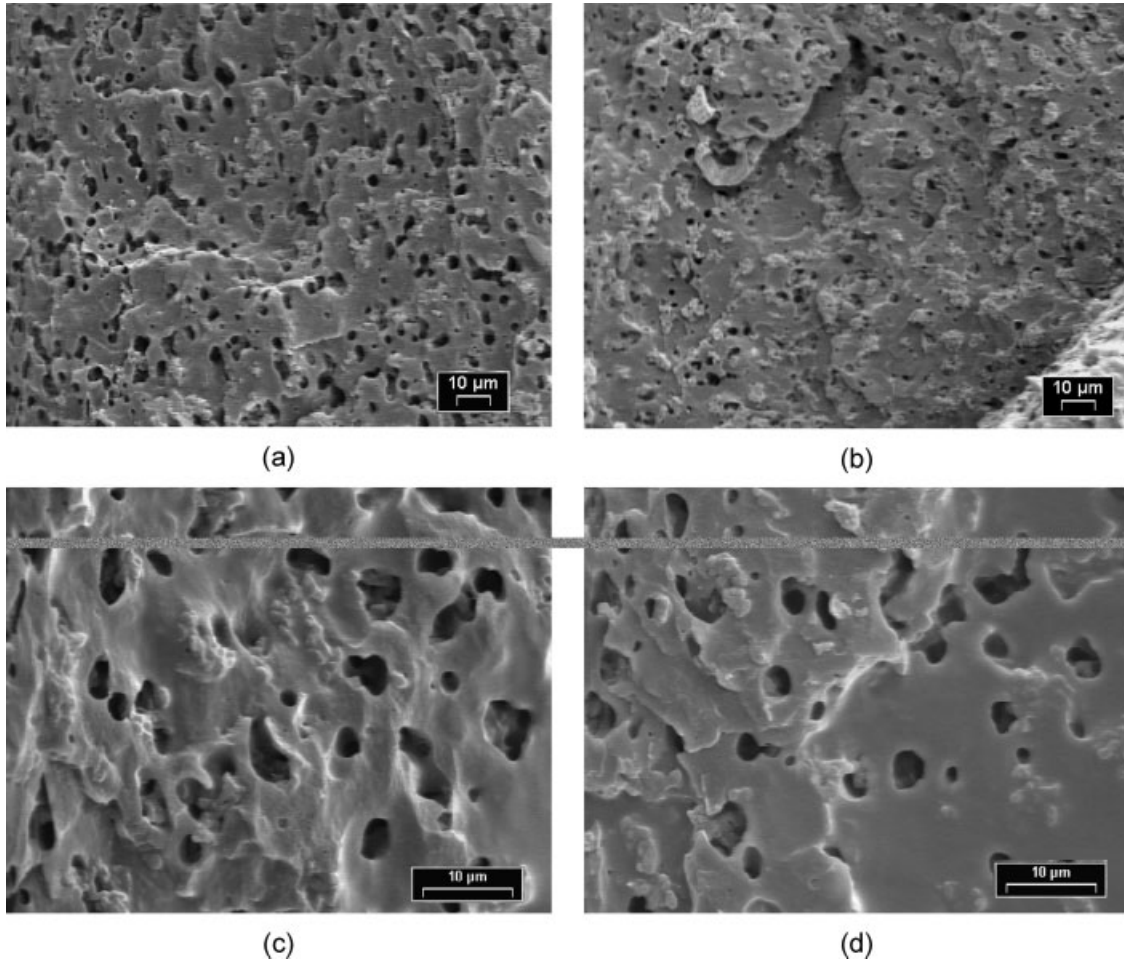
FIG. 8. SEM micrographs of a specimen of PEC subjected to a DFS followed by a DTS at 1 s^{-1} applied during 45 min at 178°C. The images were obtained at half the width and near the center of the disk (a,c) and near the external edge of the disk (b,d). Size of the observed zones: 121 × 153 μm (a,b) and 47 × 60 μm (c,d).
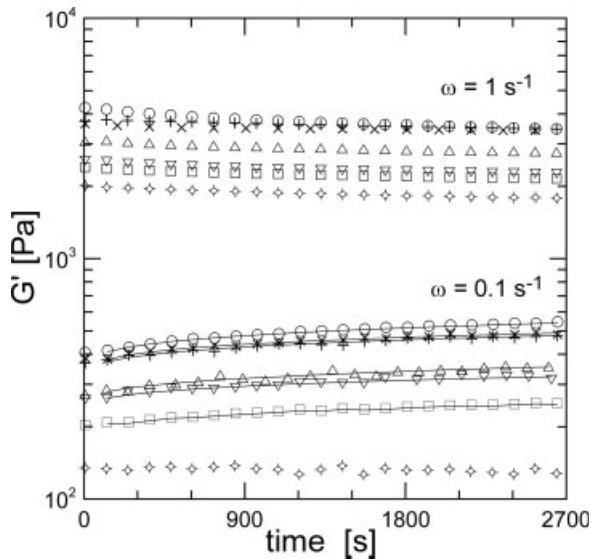

FIG. 9. Evolution of the elastic modulus of all the blends at 178°C during the dynamic time sweeps. Full lines: power-law fit of the data at 0.1 s^{-1}. PEC (○); for other symbols see Fig. 5.

time. For the cases in which the properties change, the rate of variation decreases with time and the properties approach a constant value. On the other hand, for a frequency of 1 s^{-1}, the viscous and elastic properties of all the polymers decrease with time, also approaching constant values. In both tests, PEC is the material that presents the largest rates of variation of the moduli at a given time. These rates slightly decrease as the concentration of R increases. The fact that S and R have rheological parameters that do not suffer any noticeable variation with time may be the cause of this effect. Consequently, when either S or R is added to PEC, the time dependence of the generated blends is not as significant as in the case of the original PEC. The evolution of the elastic modulus of the blends obtained during the DTS tests at 0.1 s^{-1} (which should not be substantially affected by the mechanical history) was fitted with a potential model ($G' \sim t^N$). Values of the N of 0.350 ± 0.053 were obtained. The solid lines in Fig. 9 correspond to the moduli predicted using the power-law model. It is interesting to note that, in spite of the complexity of the copolymer compositions,
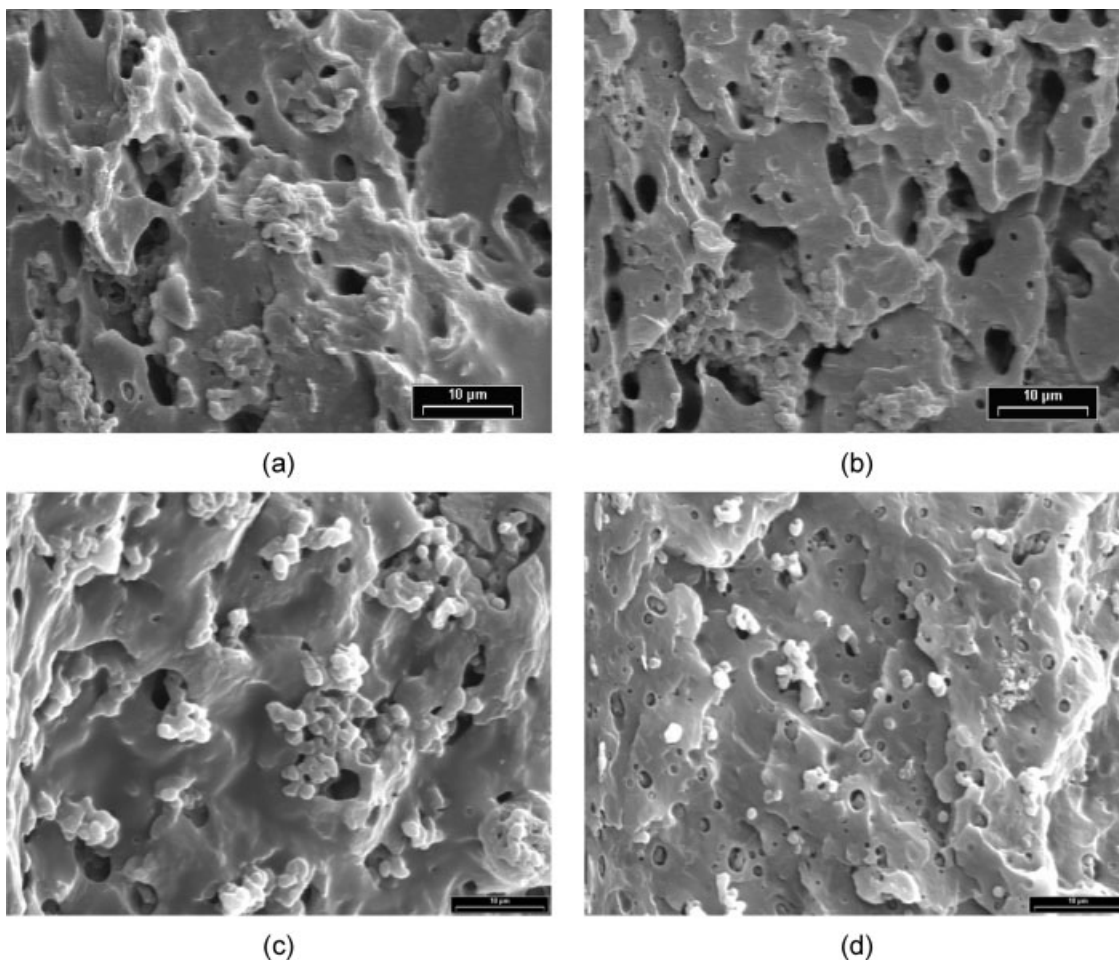
FIG. 10. SEM micrographs of the blend PEC/S0 subjected to an initial DFS at 178°C followed by 90 min at rest (a) and 45 min at 1 s^{-1} (b) and of the blends PEC/R2 (c) and PEC/R7 (d) subjected to an initial DFS at 178°C followed by 90 min at rest. Size of the observed zones: 47 × 60 μm.

this behavior is similar to the power dependence on time of the domain diameters predicted by both Ostwald ripening and the coalescence mechanisms ($d \sim t^{1/3}$) [13, 16].

The phase structure of the blends before and after the annealing process was also analyzed using SEM. All the materials show evidence of coalescence of the dispersed domains after the annealing, even PEC/R7. This effect is more important in the blends with larger concentration of S and in the samples subjected to annealing in the quiescent state. Four images are displayed in Fig. 10 to illustrate the observed morphologies. When they are compared with images in Figs. 3 and 4, the coalescence of the poly (ethylene-*co*-propylene)- and ethylene-rich areas is evident. Figure 10a and b corresponds to blend PEC/S0 after 90 min at rest and after a DTS applied during 45 min using a frequency of 1 s^{-1}, respectively. Coalescence can be appreciated in both photographs although the size of the domains seems to be slightly larger in Fig. 10a than in Fig. 10b. The phase structure of the blends PEC/R2 and PEC/R7 after 90 min at rest is shown in Fig. 10c and d (respectively). These two Figures, together with Figs. 10a and 1c, illustrate the effect of the concentration of S

on the final phase structure of the blends. As the amount of soluble material in the copolymer decreases, the size of the coalesced domains decreases when the same thermomechanical history is considered. The comparison of Fig. 10d with Fig. 4 (top) indicates that even PEC/R7 experiences coalescence during annealing.

SUMMARY

This work studies the effect of melt annealing on the phase structure and rheological behavior of a commercial propylene-ethylene copolymer (PEC) and blends of PEC and fractions obtained by toluene extraction. All the materials have approximately the same ethylene-rich material/ PP ratio and different poly(ethylene-*co*-propylene) concentrations. This concentration ranges from ~4 up to ~20 wt%. All blends showed particle-dispersion morphology after mixing in a Brabender equipment. The size and concentration of these particles increases as the concentration of rubbery material increases. Annealing in the quiescent state and with simultaneous oscillatory flow at 0.1 or 1 s^{-1} frequency was used to test the stability of the

materials at 178°C. The results obtained so far illustrate the complex behavior that multi-component polymers like propylene–ethylene copolymers may display. The morphology generated in the copolymers by the mixing conditions is thermodynamically unstable. The strong interactions between the components induce the coalescence of the domains while the polymers are kept in the molten state. Consequently, both the distribution of dispersed domains and the rheological properties gradually change in the series of materials studied. The ethylene-rich areas change in size from ∼1 to more than 10 μm of average diameter after 90 min of annealing at rest. Meanwhile, the elastic modulus practically duplicates under the same conditions. If the materials are deformed at a constant frequency during the annealing, the change in the properties is smaller. Furthermore, if the frequency is sufficiently large (1 s^{-1}), the moduli even decrease. The rheological results indicate that the applied thermo-mechanical history affects the morphology of the blends. However, no appreciable difference in phase organization was detected among the annealed samples of a given blend. Furthermore, the interphase composition, which may gradually change during annealing, may also contribute to the observed rheological changes. At present, we are extending the study to propylene-ethylene copolymers of different molecular weight and structure to analyze the effect of the viscosity and relaxation time of the components on the stability of the materials.

ACKNOWLEDGMENTS

REFERENCES

1. J. Karger-Kocsis, *Polypropylene Structure, Blends and Composites, Vol. 2: Polymers and Blends*, Chapman & Hall, London (1995).

2. E.P. Moore, Ed., *Polypropylene Handbook*, Hanser Verlag, Munich (1996).

3. R.A. Phillips and M.D. Wolkowicz, *"Structure and Morphology,"* in *Polypropylene Handbook*, E.P. Moore, Ed., Hanser Verlag, Munich, 113 (1996).

4. R. Zacur, G. Goizueta, and N. Capiati, *Polym. Eng. Sci.*, **40**, 1921 (2000).

5. L.M. Quinzani and M.D. Failla, *"Effect of the Morphology on the Rheological Properties of Propylene-Ethylene Copolymers,"* in *Research Advances In Polymer Science*, R.M. Mohan, Ed., Global Research Net Work, Kerala, India **1**, 11 (2001).

6. P. Doshev, R. Lach, G. Lohse, A. Heuvelsland, W. Grellmann, and H.J. Radusch, *Polymer*, **46**, 9411 (2005).

7. H. Tan, L. Li, Z. Chen, Y. Song, and Q. Zheng, *Polymer*, **46**, 3522 (2005).

8. Z. Fan, Y. Zhang, J. Xu, H. Wang, and L. Feng, *Polymer*, **42**, 5559 (2001).

9. L.A. Utracki, Ed., *Polymer Blends Handbook*, Kluwer Academic, Dordrecht (2002).

10. T.W. Cheng, H. Keskkula, and D.R. Paul, *J. Appl. Polym. Sci.*, **45**, 1245 (1992).

11. C.C. Chen, E. Fontan, K. Min, and J.L. White, *Polym. Eng. Sci.*, **28**, 69 (1988).

12. X.M. Xie, Y. Chen, Z.M. Zhang, A. Tanioka, M. Matsuoka, and K. Takemura, *Macromolecules*, **32**, 4424 (1999).

13. I. Fortelný and A. Zivný, *Polymer*, **36**, 4113 (1995).

14. J.G.M. Van Gisbergen and H.E.H. Meijer, *J. Rheol.*, **35**, 63 (1991).

15. L. Li, L. Chen, P. Bruin, and M.A. Winnik, *J. Polym. Sci. Part B: Polym. Phys.*, **35**, 979 (1997).

16. Y. Feng and J.N. Hay, *Polymer*, **39**, 5277 (1998).

17. T. Inoue, *"Morphology of Polymer Blends,"* in *Polymer Blends Handbook*, L.A. Utracki, Ed., Kluwer Academic, Dordrecht, 547 (2002).

18. S.B. Brown, *"Reactive Compatibilization of Polymer Blends,"* in *Polymer Blends Handbook*, L.A. Utracki, Ed., Kluwer Academic, Dordrecht, 339 (2002).

19. D. Graebling, R. Muller, and J.F. Palierne, *Macromolecules*, **26**, 320 (1993).

20. D.W. Yu, M. Xanthos, and C.G. Gogos, *J. Appl. Polym. Sci.*, **52**, 99 (1994).

21. C.B. Gell, R. Krishnamoorti, E. Kim, W.W. Graessley, and L.J. Fetters, *Rheol. Acta*, **36**, 217 (1997).

22. L.D. D'Orazio, C. Mancarella, E. Martuscelli, G. Cecchin, and R. Corrieri, *Polymer*, **40**, 2745 (1990).

23. L.D. D'Orazio and G. Cecchin, *Polymer*, **42**, 2675 (2001).

24. A.M.C. Souza and N.R. Demarquette, *Polymer*, **43**, 3959 (2002).

25. M. Kontopoulou, W. Wang, T.G. Gopakumar, and C. Cheung, *Polymer*, **44**, 7495 (2003).

26. E. Van Hemelrijck, P. Van Puyvelde, S. Velankar, C.W. Macosko, and P. Moldenaers, *J. Rheol.*, **48**, 143 (2004).

27. R.M. Paroli, J. Lara, J.J. Wheeler, K. Cole, and I. Butler, *Appl. Spectrosc.*, **41**, 319 (1987).

28. J.F. Palierne, *Rheol. Acta*, **29**, 204 (1990).

29. B. Brahimi, A. Ait-Kadi, A. Ajji, R. Jérôme, and R. Fayt, *J. Rheol.*, **35**, 1069 (1991).